Expanded View Figures

Figure EV1. Analysis of Atg4 association with the PAS by time-lapse live-cell imaging.

A Cells expressing Atg4-GFP and mCherry-V5-Atg8 (RGY287) were starved in SD-N medium for 30 min and incubated with CMAC for 10 min, before being examined by time-lapse fluorescence microscopy. PAS were considered mCherry-Atg8-positive puncta adjacent to the vacuole, stained with CMAC. Images of the same cells were collected every 1 min for 15 min. For the complete movie, see the supplemental data (Movie EV1). Scale bar, 2 μm.

B Experiments as in panel (A) were quantified by normalizing the autophagosome cycle, defined as the interval of time form the appearance until disappearance of mCherry-Atg8 puncta [49], to 1 and integrating Atg4-GFP recruitment to the PAS overtime. Data are from four independent experiments where the PAS remained in the imaged focal planes over the course of the entire filming.

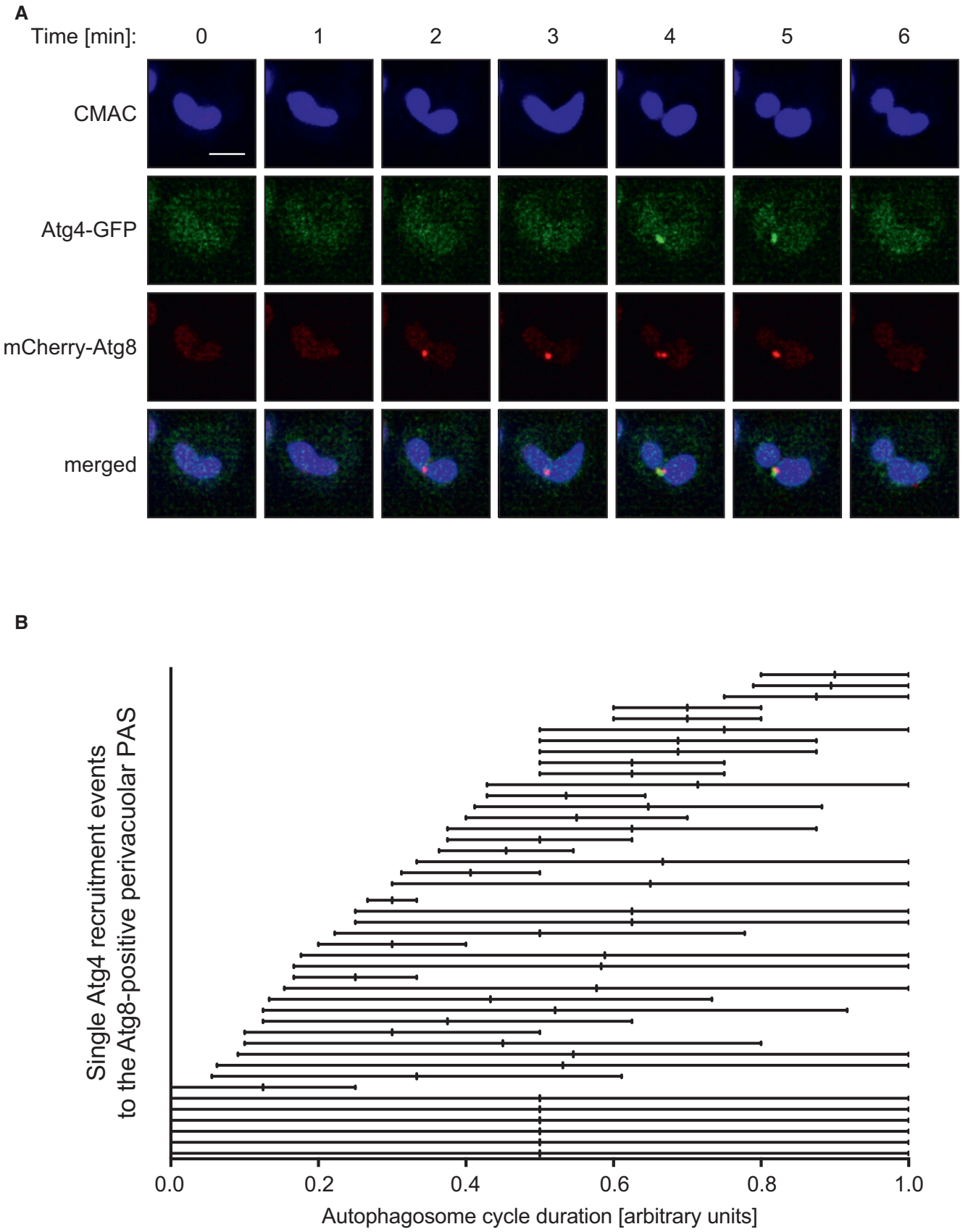

Figure EV1.

Figure EV2. Atg4 association with the PAS does not require components of the Atg1 complex, Atg9 cycling system and PI3K complex.

A Fluorescence microscopy images showing the subcellular localization of Atg4-GFP in *atg13*Δ (SAY030), *atg2*Δ (SAY109), *atg9*Δ (SAY016), *atg18*Δ (SAY017), *atg6*Δ (SAY013), and *atg14*Δ (SAY110) strains analyzed as in Fig 1. White arrows highlight Atg4-GFP puncta. DIC, differential interference contrast. Scale bars, 5 μm.

B Percentage of cells, in the experiments shown in panel (A), that display an Atg4-GFP punctate structure. Data represent the average of three independent experiments ± SD.

C Subcellular localization of Atg4-GFP in double knockout cells lacking Atg1 and components of the conjugation systems leading to the formation of Atg8-PE: *atg7*Δ (SAY032), *atg3*Δ (SAY031), *atg8*Δ (SAY033), *atg10*Δ (SAY035), *atg12*Δ (SAY134), and *atg16*Δ (SAY135). Cells were grown and imaged as in Fig 1. DIC, differential interference contrast. Scale bars, 5 μm.

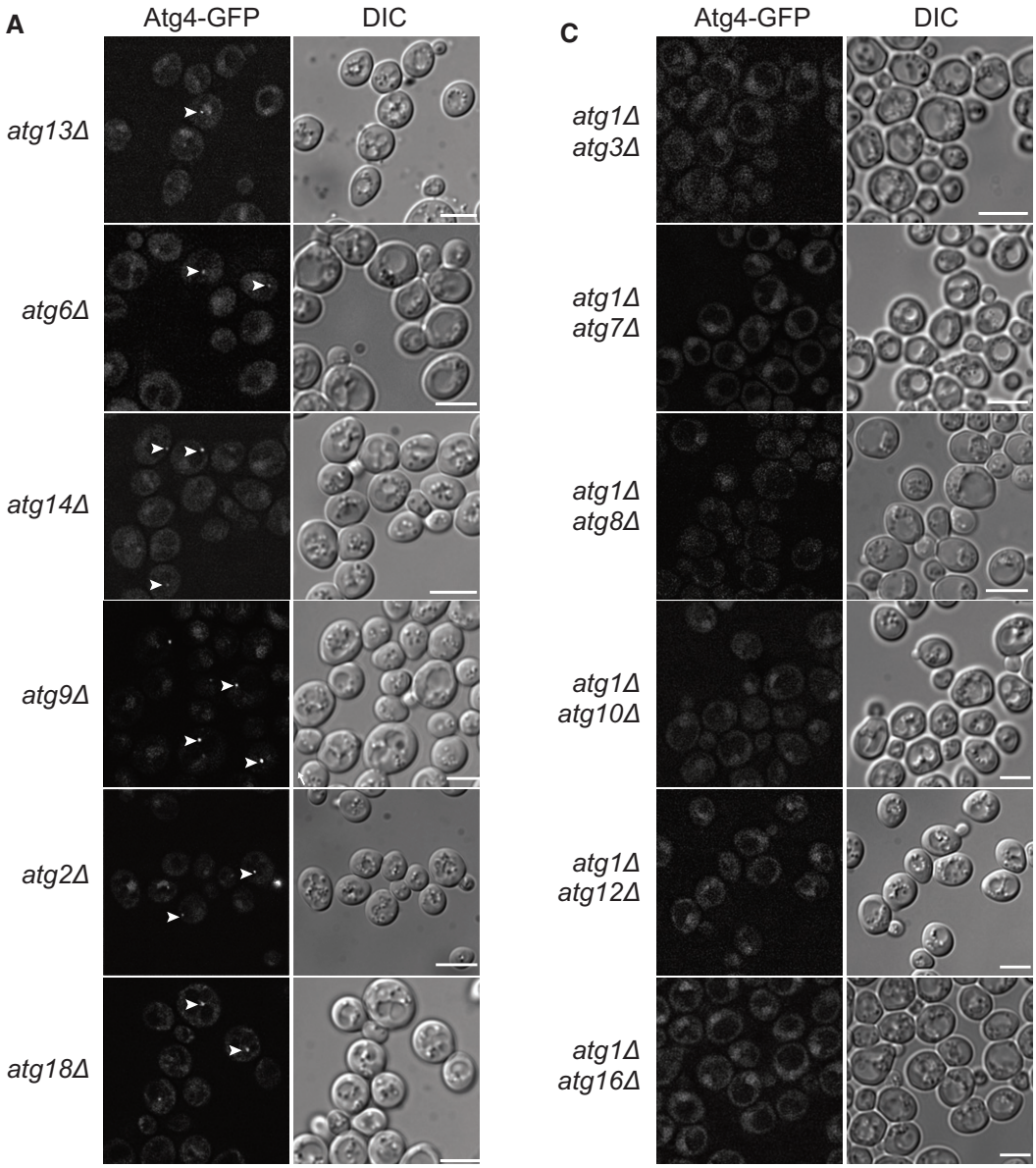

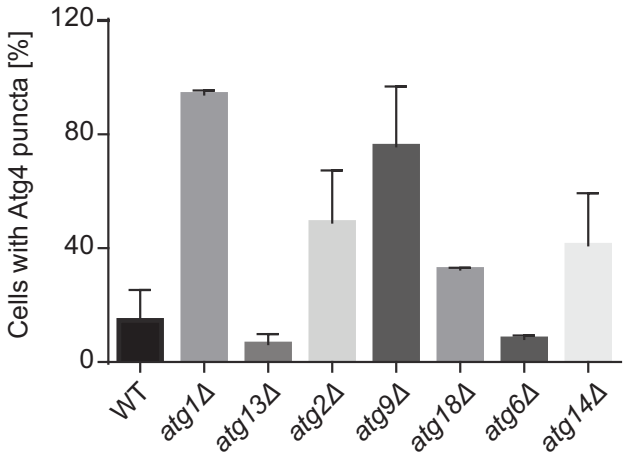

Figure EV2.

Figure EV3. Putative LIR (pLIR) motifs in *S. cerevisiae* Atg4 and their conservation among eukaryotes.

A *Saccharomyces cerevisiae* Atg4 amino acid sequence. The catalytic site (C147, D322, and H324) is highlighted in red, while the putative LIR motifs are indicated in blue.

B The amino acid sequence of the regions flanking the two conserved pLIR motifs of *S. cerevisiae* Atg4 (in blue), that is, F102 to I105 (pLIR2) and Y424 to I427 (pLIR4), were aligned with that of homologous proteins from different species using the Kalign alignment tool (http://www.ebi.ac.uk/Tools/msa/kalign/). UniprotKB accession numbers are *C. albicans* Atg4 (Q59UG3), *A. nidulans* Atg4 (Q5B7L0), *S. cerevisiae* Atg4 (P53867), *K. lactis* Atg4 (Q6CQ60), *C. elegans* Atg4.1 (Q9NA30), *C. elegans* Atg4.2 (Q9U1N6), *D. melanogaster* Atg4 (M9PBM3), *D. rerio* Atg4B (Q6DG88), *M. musculus* ATG4A (Q8C9S8), *M. musculus* ATG4B (Q8BGE6), *M. musculus* ATG4C (Q811C2), *M. musculus* ATG4D (Q8BGV9), *H. sapiens* ATG4A (Q8WYN0), *H. sapiens* ATG4B (Q9Y4P1), *H. sapiens* ATG4C (Q96DT6), and *H. sapiens* ATG4D (Q86TL0). The asterisk indicates conservation of the residue while two dots designate similarity.

A

```
1    MQRWLQLWKM DLVQKVSHGV FEGSSEEPAA LMNHDYIVLG EVYPERDEES GAEQCEQDCR
                                          pLIR1
61   YRGEAVSDGF LSSLFGREIS SYTKEFLLDV QSRVNFTYRT RFVPIARAPD GPSPLSLNLL
                                                  pLIR2
121  VRTNPISTIE DYIANPDCFN TDIGWGCMIR TGQSLLGNAL QILHLGRDFR VNGNESLERE

181  SKFVNWFNDT PEAPFSLHNF VSAGTELSDK RPGEWFGPAA TARSIQSLIY GFPECGIDDC

241  IVSVSSGDIY ENEVEKVFAE NPNSRILFLL GVKLGINAVN ESYRESICGI LSSTQSVGIA

301  GGRPSSSLYF FGYQGNEFLH FDPHIPQPAV EDSFVESCHT SKFGKLQLSE MDPSMLIGIL

361  IKGEKDWQQW KLEVAESAII NVLAKRMDDF DVSCSMDDVE SVSSNSMKKD ASNNENLGVL

421  EGDYVDIGAI FPHTTNTEDV DEYDCFQDIH CKKQKIVVMG NTHTVNANLT DYEVEGVLVE
       pLIR4                        pLIR3
481  KETVGIHSPI DEKC
```

B

	pLIR2		pLIR4	
CaAtg4	SYRCG**FEPI**PK	100	DEEEE**FINL**NV	408
AnAtg4	TYRSN**FPPI**PK	94	DEVEA**FDDL**DV	400
ScAtg4	TYRTR**FVPI**AR	107	VLEGD**YVDI**GA	429
KlAtg4	TYRTQ**FTPI**RR	82	QDTGE**YVDV**GT	401
CeAtg4.2	TYRTD**FPAL**LD	192	ADKHG**FEML**	521
MmAtg4C	TYREE**FPQI**EA	100	FSTEE**FVLL**	458
HsAtg4C	TYREE**FPQI**EG	100	FSTEE**FVLL**	458
MmAtg4D	TYRRD**FPPL**AG	133	PSSED**FVFL**	471
HsAtg4D	TYRRD**FPPL**PG	133	PSSED**FVFL**	471
CeAtg4.1	TYRRD**FSPI**GG	74	KIDDD**FEVL**DV	434
DmAtg4A	TYRHG**FSPL**GE	87	SDSDS**FAIV**ES	386
MmAtg4A	TYRRK**FSPI**GG	66	ELEED**FEIL**SV	395
DrAtg4B	TYRRK**FSPI**GG	66	DLEED**FEIL**SV	394
HsAtg4A	TYRKN**FQPI**GG	63	SEDEE**FEIL**SL	398
MmAtg4B	TYRRN**FPAI**GG	63	SEDED**FEIL**GG	393
HsAtg4B	TYRKN**FPAI**GG	63	SEDED**FEIL**SL	393
	** * :		: :	

Figure EV3.

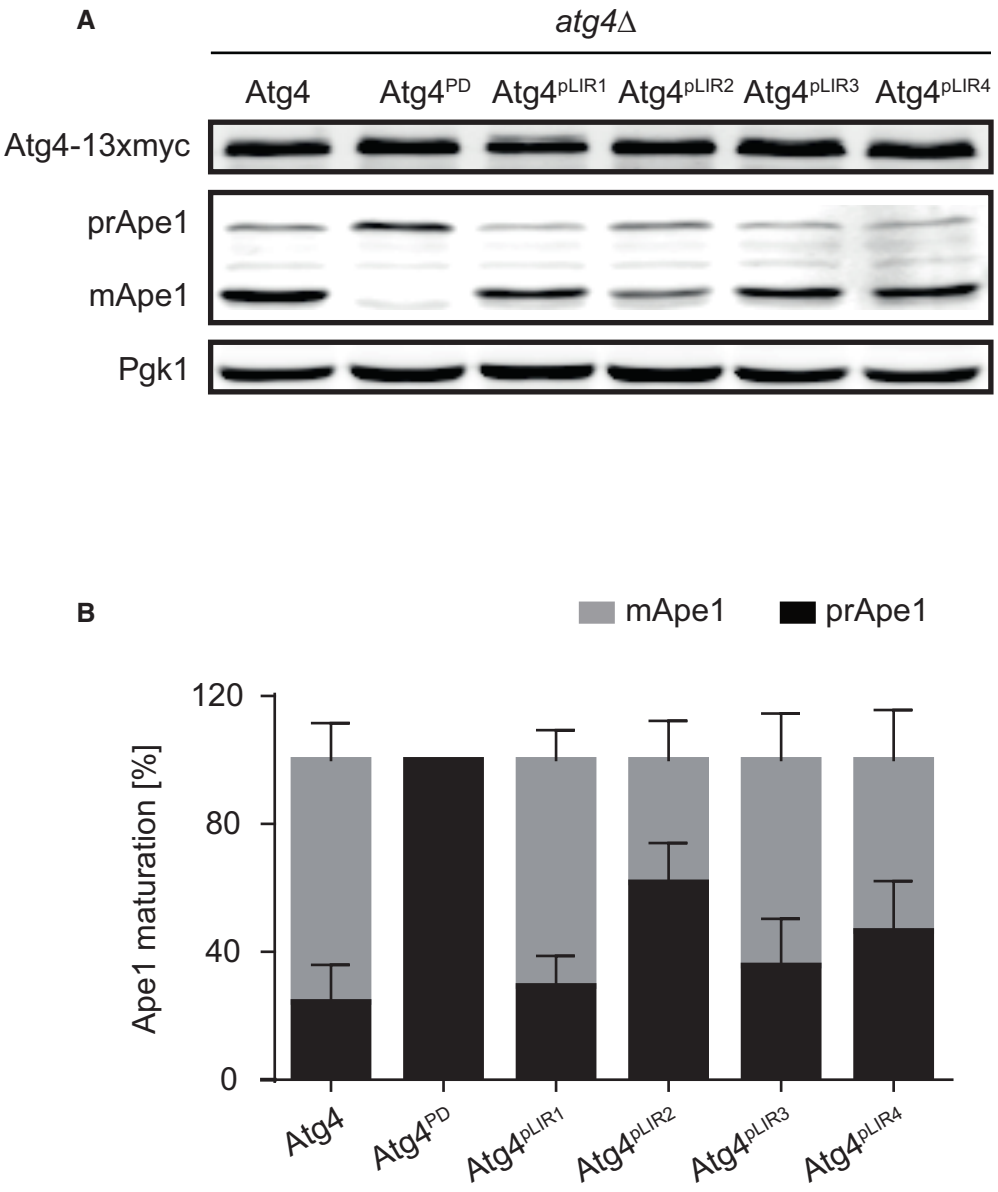

Figure EV4. Atg4 LIR2 motif is essential for the Cvt pathway.

A The strains described in Fig 2C were grown to an exponential log phase before proteins were precipitated with TCA and analyzed by Western blotting with anti-myc, anti-Ape1, and anti-Pgk1 antibodies.

B The percentage of prApe1 and mApe1 in the experiment shown in panel (A) were quantified, and values were plotted. Data represent the average of five independent experiments ± SD.